The radial electric field and its associated shear in the ASDEX Upgrade tokamak

J Schirmer, G D Conway, H Zohm, W Suttrop and the ASDEX Upgrade Team

Max-Planck-Institut für Plasmaphysik, EURATOM-Association IPP, D-85748 Garching, Germany

Abstract. The radial electric field (E_r) and its shear ($\partial E_r/\partial r$) are believed to be fundamental for turbulence suppression in magnetically confined plasmas. Doppler reflectometry offers a direct method of obtaining E_r and $\partial E_r/\partial r$ measurements. It is a type of microwave radar technique which uses the back-scatter of microwaves from a radial position in the plasma where the refractive index equals zero. In this paper, the use of Doppler reflectometry for E_r measurements is investigated. The technique is extended for $\partial E_r/\partial r$ measurements by simultaneously probing the plasma with two microwave beams at different frequencies. E_r and $\partial E_r/\partial r$ measurements are presented for a wide variety of plasma conditions. The measurements show that E_r and its associated shear are linked to plasma confinement. Their absolute values increase with confinement at the plasma edge. Furthermore, the measurements show dependence on the applied plasma auxiliary heating and the plasma shape. The E_r shear results suggest that negative shear is more influential than positive shear, in contradiction with several theoretical models.

Submitted to: *Nuclear Fusion*

PACS numbers: 52.55.Fa, 52.35.Ra, 52.70.Gw

1. Introduction

When the transition from low-confinement mode (L-mode) to high-confinement mode (H-mode) was found on ASDEX in the 1980's [1], a spontaneous bifurcation of E_r was used as a theoretical model for explaining the improved confinement. Radial electric fields and their role in plasma confinement are described in detail in review articles [2, 3, 4]. The radial electric field can be deduced from the radial force balance equation for any plasma species. For example, in the case of ions, E_r is given by

$$E_r = \frac{\nabla P_i}{q n_i} - v_{\phi_i} B_\theta + v_{\theta_i} B_\phi \tag{1}$$

where P_i, n_i, v_{ϕ_i} and v_{θ_i} are the ion pressure, ion density, ion toroidal fluid, and the ion poloidal fluid velocities. This radial electric field creates a fluid like motion known as the $E \times B$ drift given by

$$\mathbf{v}_{E\times B} = \frac{\mathbf{E} \times \mathbf{B}}{\mathbf{B}^2} \tag{2}$$

There is accumulating evidence that sheared $E \times B$ rotation is the mechanism most likely responsible for micro-turbulence suppression and confinement enhancement. The $E \times B$ flow shear reduces the plasma turbulence by nonlinear decorrelation and linear stabilization of turbulent eddies. In nonlinear turbulence decorrelation theory [5, 6], the $E \times B$ velocity shear decorrelates the turbulent fluctuations, decreases the radial correlation lengths and fluctuation amplitudes and changes the phase between density and velocity fluctuations, thereby resulting in a reduction in radial transport. In linear stabilization theory [7, 8, 9], the velocity shear can couple unstable modes to stable modes leading to transport reduction.

If the $E \times B$ velocity shear is indeed responsible for turbulence suppression, the $\partial E_r / \partial r$ may be considered as significant in quenching turbulence. This has been examined both on the experimental and theoretical front. Experiments show that at the L-H transition, an electric field shear develops in a localized region near the plasma edge [10, 11, 12, 13]. These experiments also show how in the same edge region, the turbulent density fluctuations decreased. There was also evidence of a coinciding decrease in particle and energy transport detected by an increase in the local gradients [11, 12, 14, 15]. Not only a spatial correlation between increased E_r shear, decreased density fluctuations and improved transport was observed, but also a temporal correlation [10].

In the early 1990's, several theoretical models involving E_r shear effects were also proposed. The model by Biglari, Diamond and Terry (BDT) shows how the electric field shear can nonlinearly stabilize a broad class of general, flute-like turbulent modes in the plasma [5]. The criterion for shear decorrelation to be important is when the shearing rate exceeds the decorrelation time, which can be written as

$$\left| \frac{\nabla E_r}{B_\phi} \right| > \frac{\Delta \omega_t}{k_\theta L_r} \tag{3}$$

where B_ϕ is the toroidal magnetic field, $\Delta\omega_t$ is the turbulent decorrelation frequency, L_r is the radial correlation length and k_θ is the poloidal wavenumber of the turbulence. Note that turbulence stabilization is possible for either sign of $\partial E_r/\partial r$ in this model.

Two other models which have also received attention are those by Itoh [16] and Shaing [6]. In Itoh's model, ion-orbit losses at the tokamak edge are taken into account and balanced against a non-ambipolar electron diffusion in order to derive an expression for the equilibrium radial electric field. Using this model, it was found that for a negative E_r, the shear ($\partial E_r/\partial r$) changes from small and positive in L-mode to large and negative in H-mode. This change is held responsible for the confinement improvement at the L-H transition. Shaing's model, also based on ion orbit loss theory for the generation of E_r, predicts that turbulence stabilization occurs primarily for positive E_r shear. This model balances the change in poloidal momentum against neoclassical poloidal viscous damping. It assumes that ions take up a Maxwellian distribution which may not be valid in the presence of a fast ion source such as neutral beams.

Typically, the radial electric field (and its shear) in a plasma is determined using active charge exchange spectroscopy (CXRS) and the radial force balance equation (equation 1). This method has limitations. On ASDEX Upgrade, in the absence of a diagnostic beam, the CXRS technique is dependent on neutral beam injection. This makes radial electric field measurements in purely ICRH or ECRH heated discharges very difficult. In addition, the technique usually measures the impurity velocity of say, carbon, which according to neoclassical theory is not necessarily the same as the main deuterium ion velocity. Doppler reflectometry provides an alternative method of obtaining E_r and $\partial E_r/\partial r$. The next section describes the techniques used to obtain these measurements while the following sections present experimental E_r and E_r shear measurements for a variety of plasma conditions in the ASDEX Upgrade tokamak. The results are compared with measurements from other diagnostics and with theoretical predictions. The question as to which shear, positive or negative, is more important in turbulence stabilization will be addressed.

2. Measurement Technique & Diagnostic Hardware

Doppler reflectometry was first introduced as a plasma diagnostic around 1998 for measurements of the plasma rotation velocity [17, 18]. The system differs from standard fluctuation reflectometry in that the Doppler system has tilted antennae which launch microwave beams into the plasma at a finite tilt angle θ_{tilt} with respect to the normal to the cutoff surface. The incident beams are both reflected and Bragg scattered at a corrugated cutoff layer in the plasma. For information concerning the localization of Doppler reflectometer measurements by the cut-off, see references [17, 19] for a numerical treatment and [20] for an analytic treatment. The position of the cutoff (i.e. point of reflection in the plasma) is determined as the position where the index of refraction equals zero. White has calculated analytically when this condition is met using slab

geometry [21]. For O-mode propagation, reflection occurs when

$$\omega = \frac{\omega_p}{\cos\theta_{tilt}} \tag{4}$$

where ω is the frequency of the launched microwave and $\omega_p = (ne^2/\epsilon_\circ m)^{1/2}$ is the plasma frequency. For X-mode propagation, two solutions for cutoff exist

$$\omega_R = \frac{1}{2}\left[\omega_c + \left(\omega_c^2 + 4\frac{\omega_p^2}{\cos\theta_{tilt}}\right)^{1/2}\right] \tag{5}$$

$$\omega_L = \frac{1}{2}\left[-\omega_c + \left(\omega_c^2 + 4\frac{\omega_p^2}{\cos\theta_{tilt}}\right)^{1/2}\right] \tag{6}$$

where $\omega_c = eB/m$ is the cyclotron frequency. The solutions are known as the right and left handed frequencies, ω_R and ω_L respectively.

The backscattered reflected signal from the plasma cutoff is then detected by a nearby antenna (i.e. we may assume a monostatic system). Consequently, the geometry selects the diffraction pattern of order $m = -1$. As a result, the Bragg diffraction equation gives the condition

$$k_\perp = 2k_\circ \sin\theta_{tilt} \tag{7}$$

where $k_\circ = 2\pi/\lambda_\circ$ is the probing wavenumber. Equation 7 shows that by varying the tilt angle, the Doppler reflectometer selects plasma density perturbations with finite wavenumber $k_\perp$ in the cutoff layer by the Bragg condition. Therefore, the diagnostic can provide access to the k spectrum of the turbulence.

In a fluctuating plasma, moving with velocity $u_\perp$, a Doppler shift ω_D is detected in the received microwave signal. It is given by

$$\omega_D = \vec{u} \cdot \vec{k} \tag{8}$$

For density fluctuations in tokamak plasmas, the wavenumber of the turbulence k is assumed to be perpendicular to the magnetic field B (i.e. $k_\perp$ dominates over $k_\parallel$, see [22] and references therein). Thus, the Doppler shift results only from the velocity component of the perturbations perpendicular to the magnetic field. Equation 9 gives the Doppler shifted frequency determined from the combination of equations 7 and 8.

$$f_D = u_\perp \frac{2}{\lambda_\circ} \sin\theta_{tilt} \tag{9}$$

where f_D is the Doppler shift and $\lambda_\circ$ is the wavelength of the incident microwave beam. On ASDEX Upgrade, typical values of θ_{tilt} range between 15 to 25° depending on the plasma shape. The measured Doppler shifts f_D can range anywhere between +2000 to -4000kHz, giving $u_\perp$ values between +20 to -40km/s.

The velocity $u_\perp$ contains two components:

$$u_\perp = v_{E\times B} + v_{ph} \tag{10}$$

where $v_{E\times B}$ is defined in equation 2 and v_{ph} is the phase velocity of the density fluctuation or turbulence moving in the plasma frame ($E_r = 0$). Unfortunately, there

is no direct measurement of either of these two components and thus, it is difficult to separate the two. Nevertheless there are indications from both numerical calculations and experiment that $v_{E\times B}$ dominates. Calculations with a drift wave model have shown that the phase velocity at k values in the range measured by the diagnostic (i.e. 6-8cm^{-1}) drop to a small fraction of the diamagnetic velocity [23], where the diamagnetic velocity is one component of the $E \times B$ velocity. These numerical calculations were performed for a hot, collisionless plasma with parameters typical for the edges of ASDEX Upgrade plasmas. Also, comparative measurements of Doppler reflectometer and CXRS velocities on the W7-AS stellarator show that at the plasma edge $u_\perp \approx v_{E\times B}$ during L and H-modes [17, 24]. Recently Doppler reflectometry measurements on Tore Supra also demonstrate how the $v_{E\times B}$, determined by charge exchange recombination spectroscopy, is very similar to the $u_\perp$ profile [25]. In addition, BES measurements on DIII-D resulted in a similar observation that the $E \times B$ velocity dominates over the velocity in the plasma frame (i.e. v_{ph}) [26, 27]. In JET [28], TEXT [29, 30], and TJ-II [31], experiments using probes at the plasma edge also show that the poloidal propagation velocity of the fluctuations is dominated by the $E \times B$ velocity. Hence, assuming v_{ph} is negligible, equation 10 reduces to $u_\perp \approx v_{E\times B}$, which allows the E_r to be measured:

$$E_r = -u_\perp B \tag{11}$$

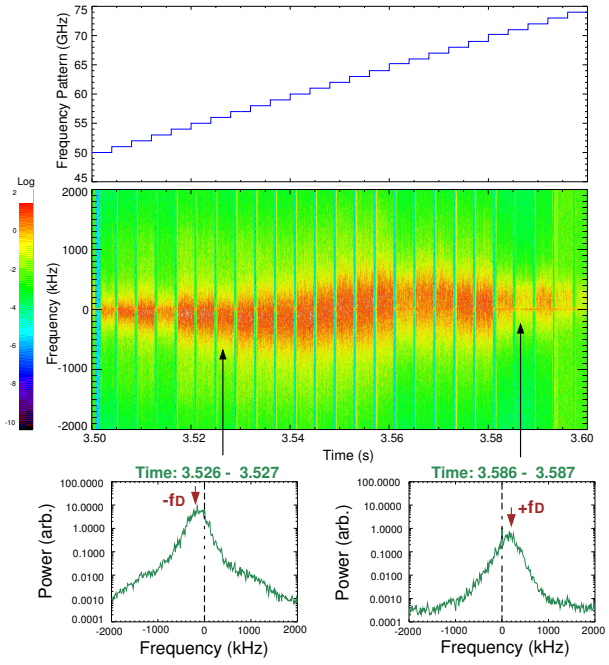

Figure 1. *Frequency spectrum showing the raw Doppler reflectometer data along with the frequency pattern used to collect the data in X-mode. The data is shown for an L-mode USN discharge # 19413 at time = 3.5s to 3.6s.*

On ASDEX Upgrade, two heterodyne Doppler reflectometers are operated in the V-band frequency range (50-74GHz). The reflectometers may launch frequencies in either O-mode and/or X-mode polarization. (Further details may be found in references

[18, 32]). Figure 1 shows an example of a typical microwave frequency launch pattern and the resulting frequency spectrum of the Doppler reflectometer data. In this example, the microwave frequency is stepped in 1GHz intervals from 50 to 74GHz over 100ms. The spectrum shows the zero frequency carrier signal as well as Doppler shifts either up or down shifted in frequency depending on the rotation direction. The change in Doppler shift is clearly illustrated by the complex amplitude signal $Aexp(i\phi)$ spectrum, two of which are shown at the bottom of figure 1. Typically, there is a narrow spike at zero frequency corresponding to the carrier wave intensity. Sometimes the m=0 direct reflection component is also observed at zero frequency as a broader, lower amplitude peak [18]. The m=-1 peak is the Doppler shifted peak which is of most interest. When the shift is large, it can be extracted by eye but when it is small, a fit routine is needed. In this case, the peak frequency is obtained by an algorithm which first removes the carrier peak, splits the spectrum into its symmetric and asymmetric components and then fits a double Gaussian to the asymmetric component using a Least-squares minimization [32].

From the measured Doppler shifts and converting the microwave probing frequencies to radial cutoff positions, a radial electric field profile versus normalized radius may be constructed. Normally, a complete profile is measured every 100ms (i.e. 1GHz steps every 4ms) to ensure that the E_r profile contains a sufficient number of data points in a short period of time. For calculating the error in the E_r measurement, a 1° error in tilt angle and a 10% error in f_D is taken. The error in the radial displacement is based on the quality of the density profile.

It should be noted that the E_r measurements as well as all other Doppler measurements presented in this paper are *local* measurements, i.e. they are measured along the antenna LOS. The plasma potential Φ is constant on the flux surface but since flux surface spacing varies poloidally, the radial electric field, which is $E_r = -\nabla\Phi$, varies with poloidal position.

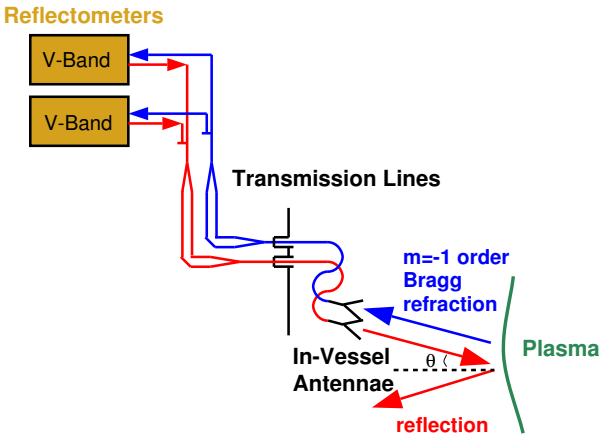

Figure 2. *Sketch of the correlation Doppler reflectometer system. The red lines indicate the transmitting path while the blue indicate the receiving path. The microwave is launched at a finite tilt angle θ with respect to the normal to the plasma cutoff surface.*

To obtain $\partial E_r/\partial r$ measurements, a correlation Doppler reflectometer system is employed. Here, two Doppler reflectometers are connected to the same antenna pair (as shown in figure 2) so that they launch microwaves with the same line of sight simultaneously into the plasma. The microwaves have different launch frequencies (f_1 and f_2) and therefore reflect from different radial positions in the plasma (r_1 and r_2). By repetitively sweeping the launch frequencies of the microwave beams with a constant fixed frequency difference, two simultaneous radial profiles of E_r can be constructed from the Doppler frequency shift in the reflectometer signal. Taking the difference between the two channels' E_r values measured at the same time divided by their radial separation gives a radial profile of the instantaneous E_r shear ($\partial E_r/\partial r$). Typically, a frequency sweep pattern of 1GHz steps from 50 to 74GHz in 100ms with a fixed 2GHz separation is used for these measurements. At the plasma edge, a 2GHz separation corresponds to approximately a 1cm radial separation.

3. Measurement of the Radial Electric Field

3.1. Dependence on Plasma Confinement

3.1.1. The L-H transition The Low to High confinement mode (L-H) transition is one of the most famous bifurcation phenomena in confined plasmas. Under the constant supply of energy, the density and temperature profiles change dramatically at the transition.

Radial electric field profiles were measured during the L-mode and H-mode phases of ASDEX Upgrade discharge #17439 ($B_\phi = -2$T, $I_p = +0.8$MA). Here positive is defined as toroidally counter-clockwise and negative clockwise when viewed from above (see figure 3(a)). Figure 3(b) shows the time evolution of typical plasma parameters during the discharge. The top time trace shows the heating power while the second trace shows the D_α line radiation intensity in the divertor indicative of the particle flux to the divertor. The L-H transition is identified at the point when the D_α line emission drops and is then followed by a series of first Type III edge localized modes (ELMs) and then Type I ELMs. The third time trace shows how the core electron density (measured by the DCN interferometer) and core electron temperature (from the ECE diagnostic) rise at the L-H transition. A significant steepening of both the density and temperature gradient at the plasma boundary is also generally observed. The last time trace shows the plasma stored energy and the H_{98} scaling factor; both being indications of the plasma confinement. The H-factor is given by

$$H = \frac{\tau_E}{\tau_{E,scaling}} \tag{12}$$

where τ_E is the measured energy confinement time and $\tau_{E,scaling}$ is an energy confinement from a scaling law. In this paper, the H_{98} factor is used for comparing confinement in the various discharges. It is calculated using the ITER scaling law [33]. The time trace shows the H_{98} factor increasing from roughly 0.6 in L-mode to 1.0 in H-mode.

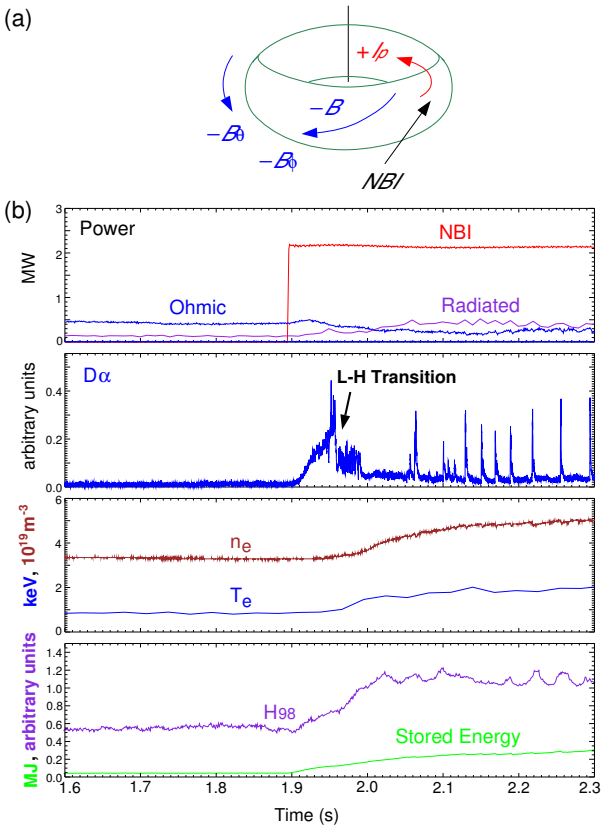

Figure 3. *(a) The standard discharge configuration on ASDEX Upgrade has left-handed helicity. In such a configuration, the ion* $\mathbf{B} \times \nabla B$ *drift points downwards. (b) The behaviour of several plasma parameters during an L-H transition in discharge #17439.*

Similarly, the plasma stored energy also increases at the L-H transition, indicating the improvement in confinement.

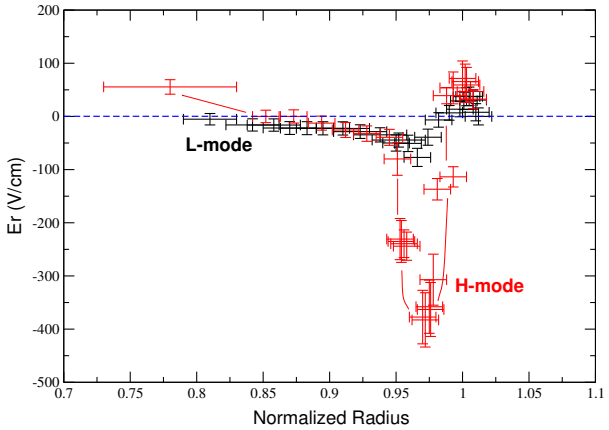

Figure 4. *Radial electric field profiles measured during an L-mode (1.9s) and an H-mode phase (2.2s) in discharge # 17439. An enhanced* E_r *is measured in the H-mode. The data was collected in O and X-mode polarization.*

Figure 4 shows the corresponding E_r profiles measured during the L-mode phase

(1.9s) of discharge #17439 shown in black and shortly afterwards in the H-mode phase (2.2s) shown in red. The E_r profiles demonstrate the high spatial resolution available with the Doppler reflectometer. The profiles are plotted versus normalized poloidal flux radius (ρ_{pol}), which is defined as

$$\rho_{pol} = \sqrt{\frac{\Psi - \Psi_a}{\Psi_s - \Psi_a}} \tag{13}$$

where Ψ is the poloidal flux and the subscripts s and a denote the separatrix and the magnetic axis respectively. Note that in the SOL (Scrape Off Layer), where ρ_{pol} is greater than one, a small positive E_r is measured. Here, E_r is determined by parallel electron losses as a result of their fast thermal motion, which drives E_r positive [34]. Then, at the plasma edge, in the pedestal region of the plasma, the E_r profile undergoes a reversal and a negative E_r well is formed. Generally, the reversal in E_r occurs at the same radial position for both L and H-mode conditions with a minimum in E_r around $\rho_{pol} \approx 0.96$. In figure 4, the E_r in the H-mode reaches a much lower minimum $[(-380 \pm 50)\text{V/cm}]$ as opposed to the minimum detected in L-mode $[(-80 \pm 20)\text{V/cm}]$. This is a typical result for all standard configuration discharges with $-B_\phi$ and $+I_p$. In such discharges, plasma edge measurements show H-mode E_r wells ranging from -300 to -450V/cm while L-mode E_r wells range from -50 to -100V/cm. Using spectroscopic measurement techniques on DIII-D [10, 35, 36], JFT-2M [14], ASDEX [37], and W7-AS [24], a sudden change in E_r at the plasma periphery during L-H transitions was also detected. The magnitudes of the edge E_r measured in L and H-modes on these devices are similar with those measured on ASDEX Upgrade using Doppler reflectometry.

3.1.2. The radial force balance The large difference in E_r between L-modes and H-modes can be understood when reviewing the radial force balance equation 1 for the ion species. One can compare the three components of equation 1 obtained by CXRS and neoclassical calculations with the E_r from Doppler reflectometry and determine which component(s) play a significant role in the edge pedestal region where the large change in E_r is observed. Figure 5 shows for discharge # 17439, the E_r, $v_{\phi_{imp}} B_\theta$, $v_{\theta_i} B_\phi$ and $\nabla P_i / q n_i$ profiles at 2.2s.

The blue solid circles in figure 5 are the toroidal impurity fluid velocity $v_{\phi_{imp}}$ multiplied by B_θ. The impurity toroidal velocity is obtained from charge exchange recombination spectroscopy (CXRS), with the C_{VI}529.05nm CX line. It is routinely measured on ASDEX Upgrade by two CXRS systems, CHR [38] and the older system CER [39, 40]. In neoclassical theory, a difference is predicted between the main ion toroidal velocity and the impurity toroidal velocity [41]. Nevertheless, it was found that in ASDEX Upgrade H-mode discharges, the neoclassical correction between main ion and impurity toroidal rotation velocities is small [42]. Only in discharges where the T_i profile becomes much steeper, should neoclassical corrections be necessary. Thus, for our purposes, the impurity toroidal velocity measured by CXRS is assumed equivalent to the main ion toroidal velocity and therefore it can be used to represent v_{ϕ_i} in equation 1. Note that in the core plasma region, E_r generally follows the $v_{\phi_{imp}} B_\theta$ term.

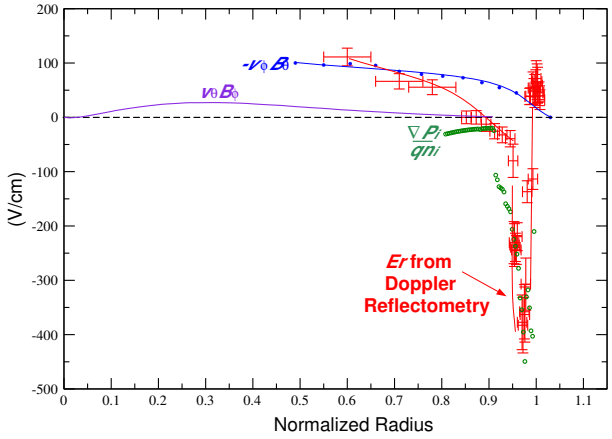

Figure 5. *The radial electric field components measured during an H-mode phase (2.2s) in discharge # 17439. E_r is determined from the Doppler reflectometer diagnostic while the toroidal velocity term is from CXRS, the poloidal velocity term from neoclassical calculations and the pressure gradient term from density and temperature measurements.*

The ion pressure P_i was also calculated for discharge #17439 using the experimental electron density profile from core Thomson scattering, profile reflectometry and DCN diagnostics (and assuming that $n_e \approx n_i$) and the experimental ion temperature profile from the charge exchange diagnostic. The pressure P_i was calculated using the relation

$$P_i = n_i T_i \approx n_e T_i \tag{14}$$

and is shown in figure 6 during the L and H-mode phases. The H-mode ion pressure

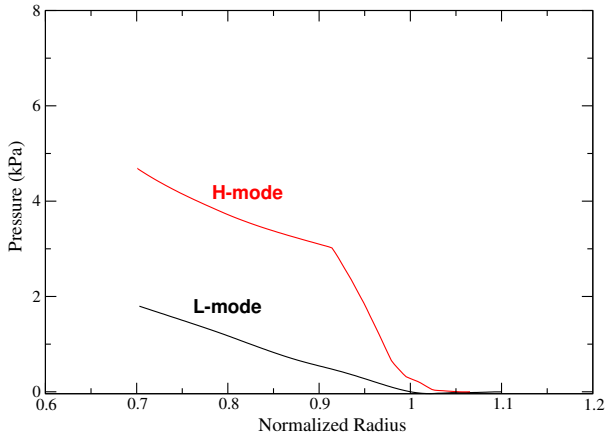

Figure 6. *Ion pressure profiles calculated using the ion temperature and electron density profiles in L-mode (1.9s) and H-mode (2.2s) phases of discharge # 17439. The H-mode pressure profile experiences a large gradient ∇P_i at the pedestal edge region in comparison to the L-mode phase.*

profile shows a steep gradient coinciding with the H-mode pedestal barrier. This is expected since the density and temperature profiles also have steep gradients in H-modes. As a result, this large pressure gradient ∇P_i causes the $\nabla P_i/qn_i$ term to

dominate the E_r profile at the plasma edge as seen in figure 5 (open circles). Hence, the large difference in E_r at the plasma edge between L-modes and H-modes could be explained by this larger pressure gradient in H-modes.

Unfortunately, poloidal velocities are not currently measured on ASDEX Upgrade and hence, no direct comparison between Doppler reflectometry and charge exchange methods of obtaining E_r are provided here. Nevertheless, an estimate of the poloidal rotation for discharge #17439 may be obtained using the neoclassical transport code NEOART [43]. The poloidal velocity multiplied by the toroidal magnetic field $v_{\theta_i} B_\phi$ is shown in figure 5 (solid line). The velocity is calculated for the deuterium ion species. The code presently does not handle the steep density and temperature gradients at the plasma edge and so the results are shown only up to $\rho_{pol} \approx 0.90$. Although it may appear that poloidal rotation plays no large role in determining E_r, CXRS measurements on other machines, such as the DIII-D tokamak, have shown that the poloidal velocity can be very high at the plasma edge, particularly at the L-H transition [35]. This high poloidal velocity is sometimes called a 'poloidal spin-up' of the plasma.

In conclusion, the E_r profile appears to be dominated by the toroidal velocity term in the plasma core whereas at the edge, the pressure gradient term is more significant. The pressure gradient appears to fully account for the large edge E_r well observed in H-modes. Unfortunately, no firm conclusion may be drawn whether the change in the E_r profile is a cause or an effect of the L-H transition. Using spectroscopic measurement techniques on other machines, a significant change in E_r right at the L-H transition was detected before the density and temperature profiles changed, suggesting that the initial change in E_r is not caused by the improved confinement [10, 11, 35]. Nevertheless, E_r may change further with the development of the profiles following the standard feedback mechanism [35, 44, 45, 46]. However, the casual role of E_r is further supported in experiments which produce H-modes by plasma biasing. In CCT [47] and TEXTOR [48] fusion devices, after the bias is applied, E_r evolves to a certain point where bifurcation occurs and the H-mode develops.

3.1.3. Improved H-modes The improved H-mode, first observed in the late nineties [49, 50], is a candidate for an *advanced tokamak* scenario. Advanced scenarios have by definition very good confinement and MHD stability properties [51]. Improved H-modes in ASDEX Upgrade have H_{98} factors around 1.2-1.4 compared with their standard H-mode counterparts with H_{98} factors around 1.0.

Figure 7 illustrates the radial electric field profiles measured in a standard H-mode phase and an improved H-mode phase. In the discharge, the data was collected by two Doppler reflectometer channels in O-mode polarization. An enhancement in E_r is detected at the edge of the improved H-mode phase. A peak value of -480V/cm is measured there while only -300V/cm is measured in the standard H-mode phase. This lower magnitude of E_r is typical of most standard H-modes on ASDEX Upgrade, as also seen in figure 4.

In this particular discharge, the electron density (from which the radial positions are

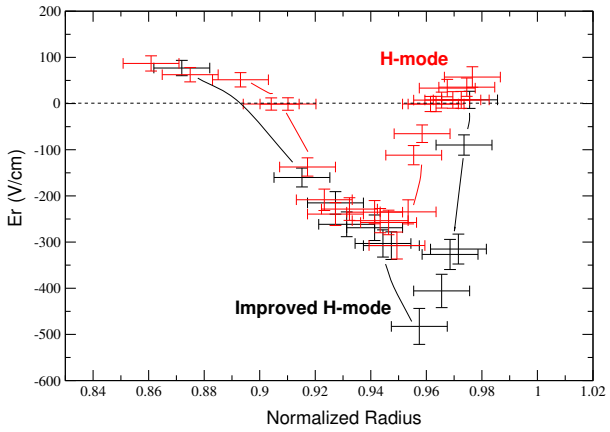

Figure 7. *Radial electric field profiles measured during a typical H-mode phase (2.9s) and an Improved H-Mode phase (4.1s) in discharge # 19112. An enhanced E_r is measured in the Improved H-mode.*

derived) was only available from DCN line interferometry and core Thomson scattering diagnostics, neither of which are optimal for edge density measurements. Hence, the radial resolution in figure 7 is poor which may explain the minor misalignment in the E_r well location between the two phases. Nevertheless, the observation that the depth of the E_r well increases with an enhancement in plasma confinement is still valid.

Figure 8 shows the time traces of plasma heating power, confinement and density in discharge # 19112. Early NBI heating is applied and a flat magnetic shear profile is maintained. Discharge # 19112 is an exceptional improved H-mode in that it was run at high density, which allows good Doppler reflectometer coverage. Also shown in figure 8 is the minimum values in edge E_r as a function of time in the discharge. The values correspond to roughly $\rho_{pol} \approx 0.95$. Note the good agreement in E_r between the two Doppler reflectometer channels. Until 3.5s in the discharge, E_r is relatively stable and then a drop in E_r occurs. The E_r well value decreases to -480V/cm, linked to an increase in confinement (H_{98}) and plasma stored energy as seen in the time traces. An impurity event at about 4.5s in the discharge causes the stored energy and confinement to drop to their lower levels and likewise, the minimum E_r also returns to its previous value of around -300V/cm. The absolute magnitude of the edge E_r does not appear sensitive to the total amount of NBI power. Its dependence on heating power will be described in a following section.

3.1.4. E_r as a function of the H_{98} Scaling Factor The experimental data indicate that the depth of the E_r well at the plasma edge increases with plasma confinement. This can be seen in figure 9 which shows for a variety of LSN (lower single null) discharges on ASDEX Upgrade the measured minimum E_r values at approximately 0.96 ρ_{pol}, coinciding with the pedestal position. The discharges have parameters in the range of I_p=0.8-1.2MA, B_ϕ=(-1.9)-(-2.7)T and n_e=2.5-8$\times 10^{19}$m$^-$3. The data is plotted versus the H/L scaling factor, H_{98}. Ohmic and L-modes have low H/L factors around 0.45 to

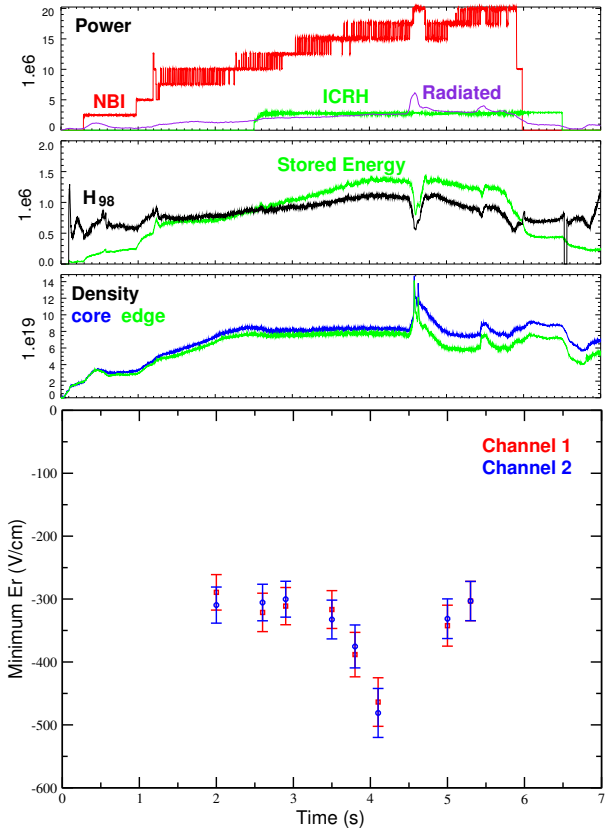

Figure 8. *The time traces of plasma parameters and the evolution of the minimum edge E_r in an improved H-mode discharge # 19112. The transition to lower E_r corresponds with an improvement in plasma confinement. The lowest E_r is measured during the improved H-mode phase.*

0.65. At this confinement, the depth of E_r is stable at about -50V/cm. At H_{98}=0.70, a bifurcation in E_r occurs as its well drops rapidly to values ranging between -250 and -350V/cm. These deeper wells are found purely in H-mode discharges. Another decrease in E_r, although less dramatic, is observed at H_{98}=1.05, marking the transition between H-modes and the higher confined improved H-modes.

The figure clearly demonstrates the relationship between the edge radial electric field and plasma confinement. The depth of the E_r well changes dramatically with confinement although no distinct variation in the width of the well is observed. The source of this enhanced E_r well appears to be related to an increase in the pressure gradient at the edge and hence a higher diamagnetic velocity $v^* = \nabla P/qnB$ contribution to E_r. (Previously, in figure 5, it was shown that at the plasma edge ∇P is the main contributor to E_r.) This explains why the depth of the E_r well is relatively stable within each scenario (i.e. Ohmic, L-mode or H-mode) where the pressure gradient is nearly unchanged within these scenarios and only undergoes a bifurcation at the L-H transition, where ∇P changes dramatically due to the steep gradients in the edge H-mode density and temperature profiles. The data in figure 9 also indicates that the edge pressure gradient should increase slightly in improved H-modes in comparison with

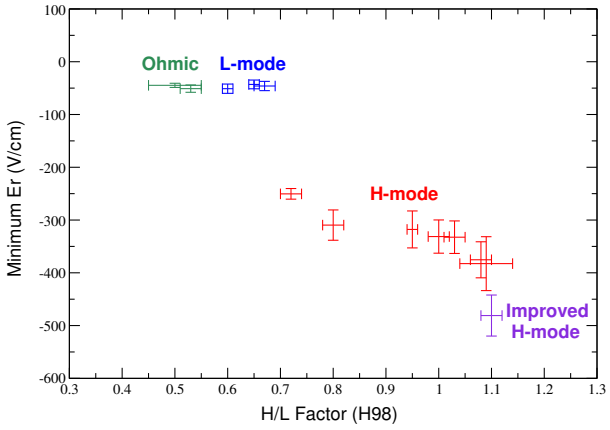

Figure 9. *The dependence of edge E_r on plasma confinement, where E_r is the minimum value and confinement is measured by the H/L factor. The data are taken from several LSN discharges between # 17439 and # 19112. A clear bifurcation in E_r is observed between L-mode and H-mode. The data was collected using O and X-mode polarization.*

standard H-modes.

3.2. Dependence on Plasma Heating

Between the H-mode and improved H-mode phases in figure 7, there is an increase in NBI heating power, from 12.4MW to 15MW. The toroidal momentum created from the tangential NBI is recognized as a driving force of the radial electric field. Hence, to determine the role of NBI heating, the behaviour of E_r in USN discharge # 19424 was examined. This discharge has a high β_N with NBI power steps ranging from 2.5MW to 10MW. As well, a constant 2.5MW of ICRH power is applied in the discharge. The time traces of several plasma parameters, including heating power, may be seen in figure 10.

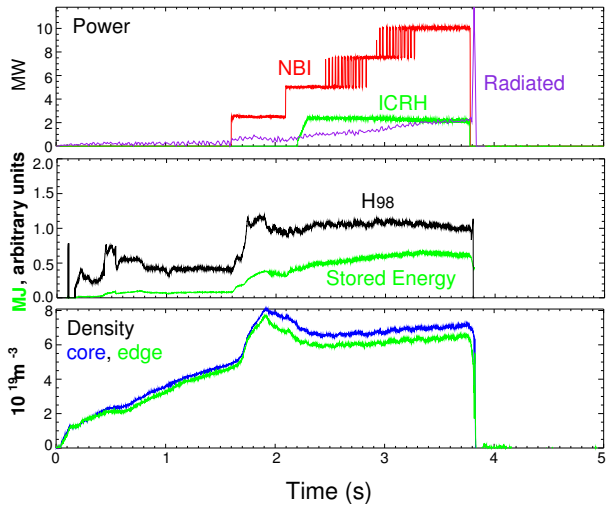

Figure 10. *The time traces of plasma parameters in discharge # 19424.*

Figure 11 shows the depth of the E_r well at $\rho_{pol} \approx 0.95$ measured in discharge # 19424 as a function of total heating power. The measurement points are all obtained in the H-mode phase with similar confinement properties. Between 2.5MW to 12.5MW total applied heating power, no significant variation in E_r is detected. The depth of E_r is stable around -200V/cm. This magnitude is smaller than typical LSN H-modes which have edge E_r values of -300V/cm. This difference arises from the dependence of E_r on plasma shape (i.e. upper single null (USN) or lower single null (LSN)) and will be discussed in the following section.

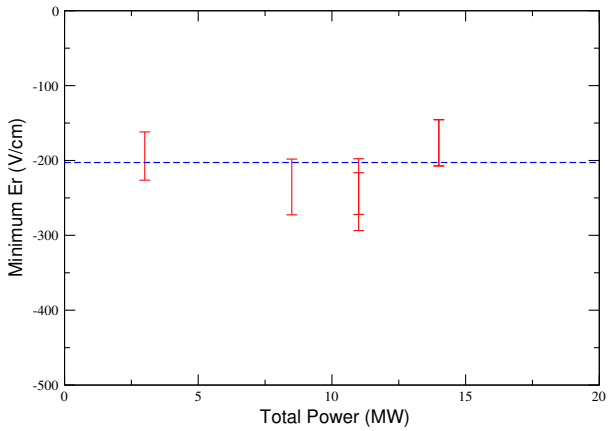

Figure 11. *The radial electric field as a function of plasma applied heating power. The data was obtained during discharge # 19424 at normalized radius $\rho_{pol} \approx 0.95$. It shows that E_r has no obvious dependence on the amount of auxiliary heating. The data was collected using O-mode polarization.*

There is a minimum input power threshold for achieving H-modes. In ASDEX Upgrade, it is given empirically by $P_{thres} = 1.75 n_e^{0.66} B_\phi^{0.71}$, where n_e is the line averaged density [52]. The critical parameter appears to be the power flow across the separatrix rather than the total heating power [53, 54]. The temperature and its gradient in a plasma are believed to be important in determining the power threshold but the ion temperature at the transition is always constant regardless of the total power [53, 55]. Hence, it appears that once the H-mode has been obtained, the total heating power is not significant in either determining the radial electric field structure in a plasma nor in determining the confinement. The observation that the minimum edge E_r remains constant in H-modes with auxiliary heating power between 2.5MW and 12.5MW confirms that the depth of the E_r well is mainly affected by changes in the edge pressure gradient, ∇P. Although the *total* amount of heating power does not appear to play a key role, this still leaves open the question whether the *type of* heating power applied affects the radial electric field.

Unlike active charge exchange spectroscopic techniques, the Doppler reflectometer diagnostic is capable of E_r measurements with all types of auxiliary heating power, e.g. NBI, ICRH and ECRH. Figure 12 compares edge E_r profiles obtained in LSN discharge #18952 ($B_\phi = +2T, I_p = -0.6MA$) using NBI and ICRH heating methods. In the discharge, between 4.8 to 4.9s, 1.6MW of pure ICRH heating is applied. At 4.95s,

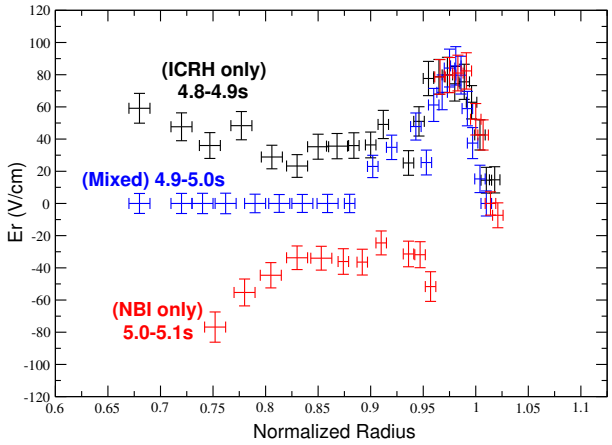

Figure 12. *Evolution of the radial electric field from an ICRH phase (4.8-4.9s) to an NBI phase (5.0-5.1s) in L-mode discharge #18952. The data was collected in X-mode polarization.*

2.5MW NBI heating is additionally applied and soon after at 5.0s, the ICRH power is switched off so that only pure 2.5MW NBI heating exists between 5.0 to 5.1s. The difference between the two heating methods is immediately evident in the E_r profiles in figure 12. Around the separatrix, the E_r profiles are positive. The E_r from the phase with NBI heating (shown in red) then becomes negative as the diamagnetic velocity (i.e. the main contributor to E_r at the plasma edge) is positive (note the B dependence in the diamagnetic velocity). In the plasma mid-core, the E_r remains negative as the poloidally mapped toroidal velocity $v_\phi B_\theta / B$ (i.e. the main contributor to E_r in the plasma core) is positive in reversed B_ϕ, I_p discharges. (Note that on ASDEX Upgrade, by reversing I_p, the NBI heating is counter-current injected.) The overall plasma rotation with pure NBI heating is in the counter-current direction. However, when pure ICRH heating is applied, the measured E_r (shown in black) becomes positive in the plasma mid-core, indicating that a negative toroidal rotation exists there. The overall plasma rotation is now in the co-current direction. This result agrees with observations from JET [56] and Alcator C-Mod [57] in which plasmas rotate in the co-current direction with ICRF as the sole additional heating. The mechanism for the observed co-rotation is still unresolved but several theories associated with large drift orbits exist [58].

A combination of both heating power methods (shown in blue) results in a cancellation of the radial electric field in the plasma mid-core. Previous experimental measurements on ASDEX Upgrade, using the charge exchange diagnostic, have shown that ICRH heating causes a reduction of v_ϕ driven by NBI in the co and counter-current directions [42]. A reduction in v_ϕ by a factor of two in counter-NBI discharges is detected and is attributed to an increasing momentum diffusivity connected with the confinement degradation by the additional ICRH power flux [42]. (Confinement degradation is the same mechanism used to explain the reduction in v_ϕ due to pure electron heating with ECH in DIII-D [59].)

3.3. Dependence on Plasma Shape

Another factor which is known to affect confinement and hence the radial electric field is the shape of the plasma [61]. In a pure 1.3MW ICRH heated discharge # 19415 ($B_\phi = -2T, I_p = +0.8MA$), the plasma shape was altered from lower single null (LSN) to double null (DN) and then to upper single null (USN).

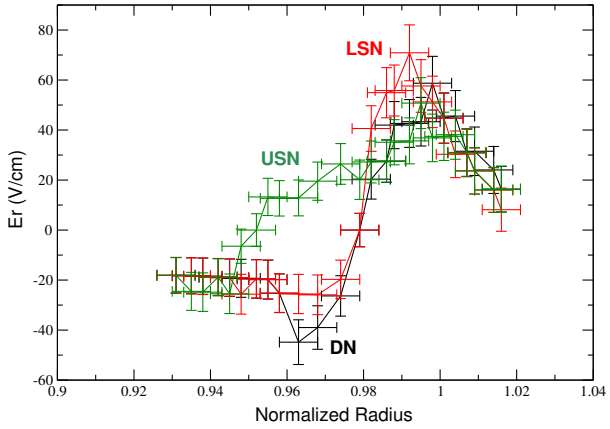

Figure 13. *The radial electric field profiles of discharge # 19415 measured during various plasma shapes: LSN (3.0s), DN (4.4s), USN (5.8s). The absolute E_r and its shear are smaller in USN shaped plasmas. The data was collected in X-mode polarization.*

Figure 13 shows the E_r profiles with L-mode conditions for the three plasma shapes. A positive radial electric field is measured in the SOL/separatrix region in all profiles due to the fast open flux surface connection to the divertor but, the formation and depth of the E_r well around the pedestal depends strongly on the plasma shape. The DN configuration has the lowest edge E_r of -44.8V/cm at $\rho_{pol} = 0.96$, followed by the LSN configuration with -25.6V/cm at the same position. The E_r measured in the USN configuration, however, is still positive at the plasma edge at $\rho_{pol} = 0.96$ and only makes the transition to negative E_r at $\rho_{pol} = 0.95$.

The behaviour observed can be explained by the impact the divertor configuration has on the parallel fluxes in the plasma. Rozhansky et al. has undertaken modeling of the radial electric field in discharge # 19415 for the three plasma shapes using a B2SOLPS5.0 transport code [60]. It was found that the geometrical configurations change mainly the distribution of the parallel fluxes in the SOL and through an anomalous viscosity change the parallel fluxes in the viscous layer (i.e. the layer just adjacent to the separatrix where E_r changes in the three plasma shapes). There are three contributions to the parallel fluxes in the SOL: the Pfirsch-Schlueter (PS) flux (which closes the vertical ∇B drift of ions), the flux compensating the $\mathbf{E} \times \mathbf{B}$ drift in the radial electric field, and the parallel unbalanced flux (which is directed to the divertor target plates). The simulations show that in upper single null shaped plasmas, the divergences of the vertical ∇B drift flux and parallel fluxes is smaller than in lower single null and double null shaped plasmas. This may account for the difference in E_r

and its shear being small in USN shaped plasmas, as seen in the experiment.

The change in E_r with plasma shape may also account for the differences in confinement in the respective shapes. The USN shape, with the smallest E_r well, has the lowest confinement (0.65 H_{98}) while during LSN and DN configurations, the plasma has H_{98} factors of 0.70. Figure 9 shows that the change in the depth of the E_r well is greatest between 0.67 and 0.72 H_{98} factors.

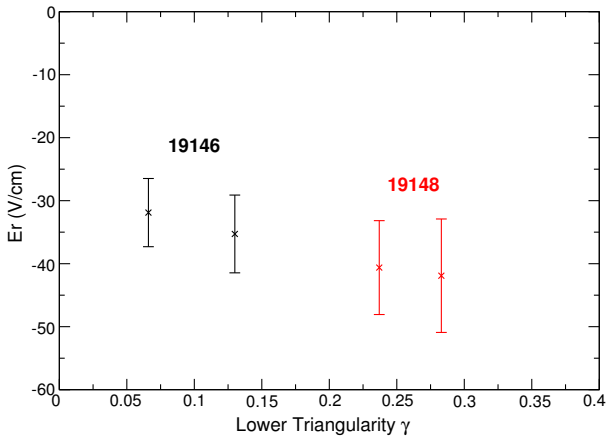

Figure 14. *E_r as a function of lower triangularity for the pair of USN L-mode discharges # 19146, # 19148. The data was collected in X-mode polarization.*

To further study the role of plasma shape on E_r, a triangularity ramp was performed in two USN L-mode discharges # 19146 and # 19148. All plasma parameters were held approximately constant in these discharges. Figure 14 presents the relationship of E_r with plasma triangularity. The E_r shows a slight dependence on this quantity, decreasing with triangularity. A slight improvement in the H_{98} factor with triangularity is also observed in these discharges. Measurements on JET and DIII-D show that the confinement time in a plasma depends strongly on plasma shape, improving with triangularity [61, 62]. The experimental results presented here offer supporting evidence of this observation.

4. Measurement of the Radial Electric Field Shear

4.1. Experimental Measurements

In the fundamental transport equations, all direct radial electric field effects cancel and transport effects enter only through the derivatives of E_r (i.e. its shear) [4]. Hence, the shear in E_r may be of greater importance in tokamak physics than E_r itself, especially in the stabilization of turbulence. On the TEXTOR tokamak, experiments with Langmuir probes showed the largest reduction of turbulence transport at the location of the highest electric field gradient [63]. It was also observed that density fluctuations are sensitive to the sign of the E_r shear [63]. Using the correlation Doppler reflectometer system sketched in figure 2, measurements of $\partial E_r/\partial r$ were made on ASDEX Upgrade and are presented here for various plasma scenarios.

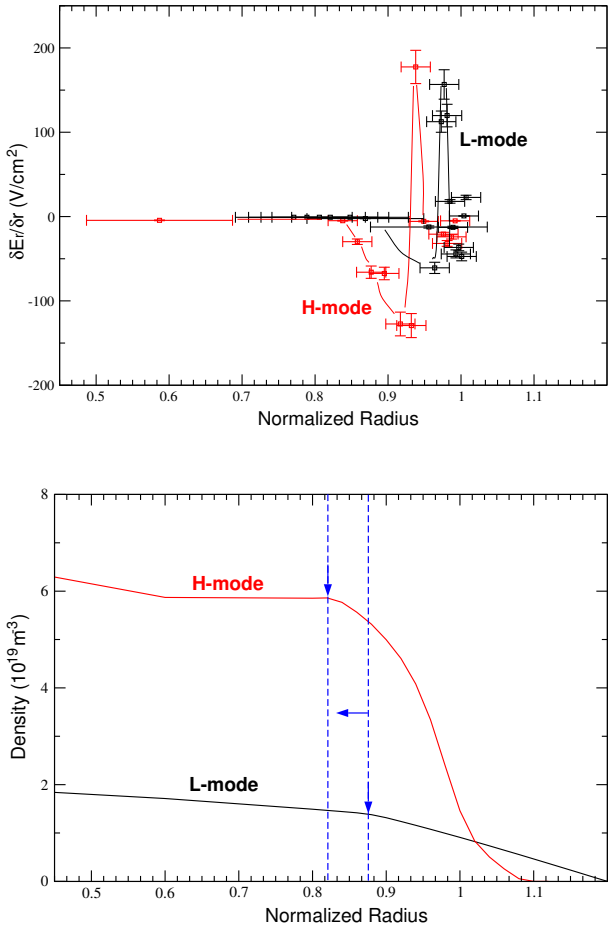

Figure 15. *The radial electric field shear measured during L-mode discharge (# 18103) using X-mode polarization and H-mode discharge (#17973) using O-mode polarization. The experimental electron density profile steepens and moves inwards during an H-mode, accounting for the radial shift in the E_r shear profiles.*

Figure 15 presents the radial electric field shear measured in an L-mode (# 18103 at 3.7s) and H-mode (# 17973 at 6.0s) LSN discharge. In both discharges, the two channels of the correlation Doppler reflectometer had a similar frequency launch pattern: 1GHz steps from 50 to 74GHz in 100ms with a 2GHz fixed frequency difference between the two channels. In the L-mode discharge, the data was obtained using X-mode polarization while in the H-mode discharge, O-mode polarization was used. The polarization was chosen for edge measurements in both discharges.

In comparing the shear measured in the two discharges, three observations can be made. First, the shear is localized at the plasma edge and almost zero elsewhere. It has both a positive peak and a negative well. Second, the H-mode E_r shear profile is shifted inwards in comparison to the L-mode profile. This may be due to the density pedestal which steepens and moves inwards during an H-mode [64]. This is seen when comparing the experimental density profiles obtained by DCN, standard reflectometry and core

Thomson scattering diagnostics in both discharges. The third observation is that the absolute value of the edge E_r shear increases after the L-H transition. Typically at ASDEX Upgrade the maximum negative edge E_r shear measured in L-modes is between 0 and -75V/cm^2 and in H-modes between -150 and -250V/cm^2. This enhanced shear in H-mode is observed for all types of H-modes, i.e. NBI heated, ICRH, etc. Similar values of E_r shear in L-modes and H-modes were obtained on DIII-D using charge exchange recombination spectroscopy [65].

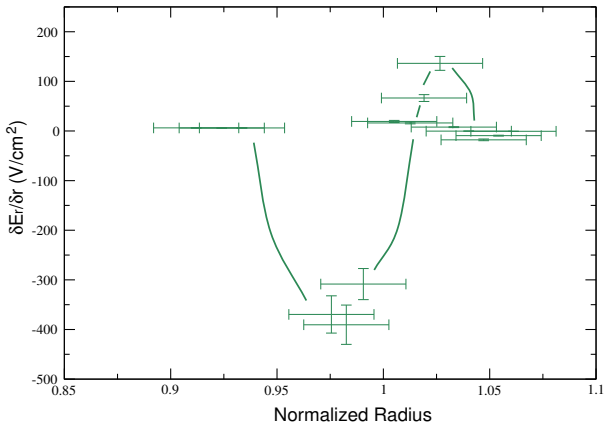

Figure 16. *The radial electric field shear measured during a quiescent H-mode discharge # 18925 at 3.5s. The largest absolute E_r shear measured on ASDEX Upgrade to date has been during the quiescent H-mode discharges. The data was collected with X-mode polarization.*

Figure 16 shows the shear measured during a quiescent H-mode phase. The quiescent H-mode phase, like the ELMy H-mode, has very high confinement but is ELM-free. In ASDEX Upgrade, the highest shear measured to date has been during the quiescent H-mode phase. It has been suggested by Burrell [66] that the strong shear (greater than -400 V/cm^2) in this plasma regime may be an explanation for the observed ELM stabilization.

4.2. Discussion

All measurements in ASDEX Upgrade indicate that the positive shear peak at the plasma edge is relatively constant ($\approx$ +150 to +200V/cm^2) for a variety of discharges. This shear is associated with the plasma separatrix/SOL region. It is rather the negative shear peak, linked to the plasma pedestal region, that appears more important, with changes ranging from almost zero to -400V/cm^2. In Itoh's model, the shear flips from small and positive in L-mode to large and negative in H-mode and it is the jump in E_r shear which is proposed as being responsible for confinement improvement [16]. The small negative shear in L-modes which are observed in the Doppler reflectometer measurements are not accounted for in Itoh's model. In Shaing's model, turbulence stabilization occurs primarily for E_r shear greater than zero [6]. Again, this model does not represent the experimental E_r shear measurements since the role of the negative

shear is dominant. The Biglari, Diamond and Terry (BDT model) predict that an increase in absolute shear suppresses density fluctuations and stabilizes the turbulence [5]. Turbulence stabilization may occur for either sign of $\partial E_r/\partial r$ in this model. The data shown in figure 15 is consistent with their model.

The BDT model also describes a criterion for shear decorrelation given in equation 3. Typical values of turbulence parameters observed at ASDEX Upgrade are $\Delta\omega_t$=2.5 $\times$ $10^5 s^{-1}$, L_r=0.5cm and k_θ =1cm^{-1} [67]. With a magnetic field B_ϕ=2T, the BDT criterion is satisfied when $|\nabla E_r| > 100 V/cm^2$. The measured magnitudes of E_r shear on ASDEX Upgrade are large enough to satisfy this criterion. However, it should be noted that the turbulence parameters are only estimates and hence the $100 V/cm^2$ boundary is an approximation. Reference [67] gives further estimates when the BDT criterion is met on JET and DIII-D.

In figures 15 and 16, the large extent of the shear layer is illustrated. One would expect that the width of the shear layer is of the order or larger than the size of a turbulent eddy ($\approx$ 1cm) in order to be effective for turbulence suppression. On DIII-D, E_r shear layers in H-mode plasmas range between 3.20 to 4.80cm [36] while on JFT-2M, H-mode plasmas have shear velocity layers with widths ranging between 2.2 to 3.6cm [68]. The width of the negative E_r shear layer measured in H-mode on ASDEX Upgrade as shown in figure 15 is 5.2cm. This large radial extent of the E_r shear is certainly sufficient for effective turbulence suppression.

5. Summary

Radial electric field and shear measurements were performed on ASDEX Upgrade using the newly developed correlation Doppler reflectometer system. Both these parameters, E_r and $\partial E_r/\partial r$, are thought to play a major role in the suppression of plasma turbulence and hence their measurements are much sought after. Generally, the radial electric field in a plasma is measured using active charge exchange spectroscopy (CXRS) and the radial force balance equation. This method relies on accurate poloidal and toroidal rotation measurements from CXRS as well as accurate electron or ion densities and temperatures for calculation of the electron or ion diamagnetic velocity. Due to the strong gradients in density and temperature at the plasma edge, accurate measurements are difficult to achieve and diagnostics need to be specially developed for such measurements. The Doppler reflectometer can by-pass all these obstacles since the perpendicular velocity which it measures is directly related to E_r. By using a second Doppler reflectometer channel (i.e. correlation Doppler reflectometry), the measurement of instantaneous E_r shear is possible.

The E_r profile in a standard ASDEX Upgrade plasma configuration, with $-B_\phi, +I_p$, is positive in the SOL and then undergoes a reversal at the plasma edge, coinciding with the plasma pedestal region. This reversal forms what is known as an E_r well. The depth of the well is observed to increase dramatically with the confinement of the discharge (see figure 9) while the width of the well appears unaffected. The edge pressure gradient

∇P is most likely the influential factor in determining the depth of the E_r well. The pressure gradient becomes steeper at the edge in H-mode (in comparison with L-mode and ohmic discharges) due to the steeper gradients in density and temperature. Once an H-mode is obtained, the amount of total auxiliary heating power does not affect the E_r well depth. This supports that ∇P, which remains relatively constant in H-modes, is the influential factor in determining the depth of the E_r well. ∇P is limited by MHD stability criterion, that is, a certain edge current density can only support a certain plasma pressure otherwise it becomes kink unstable. The E_r profile, however, is altered by the type of heating power applied. In counter-current pure NBI heated discharges, $v_\phi B_\theta$ is in the counter-current direction while in pure ICRH heated discharges, it is in the co-current direction. Hence, the E_r profiles in figure 12 have opposite signs. The results indicate that ICRH heating may drive toroidal rotation, although when it is added to NBI heating, it reduces v_ϕ. This reduction can be explained by an increase in momentum diffusivity connected with the confinement degradation by the additional ICRH power flux [42]. The dependence of E_r on plasma shape was also investigated. It was found that the shape does have a strong influence on the edge E_r profiles. USN shaped plasmas have smaller absolute E_r magnitudes than LSN shaped plasmas. Simulation work by Rozhansky has shown that the divertor configuration changes the parallel fluxes in the SOL and edge, which may explain the difference in E_r [60].

The E_r shear measurements have shown the importance of accurate electron density measurements since $\partial E_r/\partial r$ depends heavily on radius r. The E_r shear profiles are localized at the plasma edge, being small elsewhere. Measurements in L-modes, H-modes and quiescent H-modes show that the positive shear at the plasma edge is relatively constant but the degree of negative shear increases with plasma confinement. The negative shear ranges between 0 and -75V/cm^2 in L-modes, -150 to -250V/cm^2 in H-modes and -400 to -500V/cm^2 in QH-modes. In comparing the experimental measurements to the global aspects of various theories about E_r shear, it was found that the BDT model agrees best with the trend observed in the measurements. Both the magnitude of the E_r shear and its radial extent are large enough to suppress fluctuations according to the BDT model.

Acknowledgments

Dr.Yong-Su Na is acknowledged for fruitful discussions concerning improved H-modes, Dr. Frank Jenko and Dr. Bruce Scott for useful discussions regarding the radial electric field shear measurements and Dr.Ralph Dux for providing poloidal rotation data from neoclassical calculations, using the NEOART code.

References

[1] Wagner F *et al* 1982 *Phys. Rev. Lett.* **49** 1408
[2] Itoh K *et al* 1996 *Plasma Phys. Control. Fusion* **38** 1
[3] Burrell K H 1997 *Phys. Plasmas* **4** 1499

[4] Ida K 1998 *Plasma Phys. Control. Fusion* **40** 1429
[5] Biglari H *et al* 1990 *Phys. Fluids* **B2** 1
[6] Shaing K C *et al* 1990 *Phys. Fluids* **B2** 1492
[7] Staebler G M *et al* 1991 *Nucl. Fusion* **31** 1891
[8] Hassam A B *et al* 1991 *Comments Plasma Phys. Control. Fusion* **14** 275
[9] Carreras B A *et al* 1992 *Phys. Fluids* **B4** 3115
[10] Burrell K H *et al* 1992 *Plasma Phys. Control. Fusion* **34** 1859
[11] Doyle E J *et al* 1991 *Phys. Fluids* **B3** 2300
[12] Groebner R J *et al* 1991 *Plasma Physics and Controlled Nuclear Fusion Research 1990 (Proc.* 13^{th} *Int. Conf. Washington DC, 1990)* **1** 453, IAEA, Vienna
[13] Matsumoto H *et al* 1992 *Plasma Phys. Control. Fusion* **34** 615
[14] Ida K *et al* 1990 *Phys. Rev. Lett.* **65** 1364
[15] Ida K *et al* 1992 *Phys. Fluids* **B4** 1360
[16] Itoh S I *et al* 1990 *J. Phys. Soc. Japan* **59** 3815
[17] Hirsch M *et al* 2001 *Plasma Phys. Control. Fusion* **43** 1641
[18] Conway G D *et al* 2004 *Plasma Phys. Control. Fusion* **46** 951
[19] Bulanin V V *et al* 2002 *Proc. 29th EPS Conf. on Controlled Fusion and Plasma Physics (Montreux)* **26B** P-2.121
[20] Gusakov E Z *et al* 2004 *Plasma Phys. Control. Fusion* **46** 1143
[21] White R B *et al* 1974 *Plasma Physics* **16** 565
[22] Liewer P C *et al* 1985 *Nucl. Fusion* **25** 543
[23] Scott B 2001 Low frequency fluid drift turbulence in magnetised plasmas *Report* IPP 5/92, Max-Planck-Institut für Plasmaphysik, Garching
[24] Hirsch M *et al* 2006 *Plasma Phys. Control. Fusion* **48** S155
[25] Hennequin P *et al* 2005 Proceedings of the 7^{th} International Reflectometry Workshop for Fusion Plasma Diagnostics (IRW7) *Report* IPP 2/9, Max-Planck-Institut für Plasmaphysik, Garching
[26] McKee G R *et al* 2000 *Phys. Plasmas* **7** 1870
[27] Jakubowski M *et al* 2001 *Rev. Sci. Instrum.* **72** 996
[28] Gonçalves B *et al* 2001 *Czech. J. Phys.* **51** 995
[29] Ritz Ch P *et al* 1990 *Phys. Rev. Lett.* **65** 2543
[30] Ritz Ch P *et al* 1984 *Phys. Fluids* **27** 2956
[31] Hidalgo C *et al* 2004 *Phys. Rev.* **E70** 067402
[32] Klenge S 2005 *Dynamik magnetisch eingeschlossener Plasmen am L-H Übergang*, PhD Thesis, Universität Stuttgart, Germany
[33] ITER Physics Basis 1999 *Nucl. Fusion* **39** 2137
[34] Baldzuhn J *et al* 1998 *Plasma Phys. Control. Fusion* **40** 967
[35] Groebner R J *et al* 1990 *Phys. Rev. Lett.* **64** 3015
[36] Moyer R A *et al* 1995 *Phys. Plasmas* **2** 2397
[37] Field A R *et al* 1992 *Nucl. Fusion* **32** 1191
[38] Maggi C F *et al* 2003 30^{th} *EPS Conference on Controlled Fusion and Plasma Physics* P1.63
[39] Kallenbach A *et al* 1990 *Nucl. Fusion* **30** 645
[40] Meister H *et al* 2001 *Nucl. Fusion* **41** 1633
[41] Kim Y B *et al* 1991 *Phys. Fluids* **B3** 2050
[42] Nishijima D *et al* 2005 *Plasma Phys. Control. Fusion* **47** 89
[43] Peeters A G 2000 *Phys. Plasmas* **7** 268
[44] Burrell K H *et al* 1990 *Phys. Fluids* **B2** 1405
[45] Field A R *et al* 1991 *Proc.* 18^{th} *European Conf. on Controlled Fusion and Plasma Physics, Berlin* **15C** Part III, 113
[46] Groebner R J *et al* 1992 *Proc.* 19^{th} *European Conf. on Controlled Fusion and Plasma Physics, Innsbruck* **16C** Part I, 183
[47] Taylor R J *et al* 1989 *Phys. Rev. Lett.* **63** 2365

[48] Weynants R R *et al* 1991 *Plasma Physics and Controlled Nuclear Fusion Research 1990 (Proc. 13th Int. Conf. Washington DC, 1990)* **1** 473, IAEA, Vienna
[49] Gruber O *et al* 1999 *Phys. Rev. Lett.* **83** 1787
[50] Wolf R C *et al* 1999 *Plasma Phys. Control. Fusion* **41** B93
[51] Taylor T S 1997 *Plasma Phys. Control. Fusion* **39** B47
[52] Ryter F *et al* 2002 *Plasma Phys. Control. Fusion* **44** A415
[53] Carlstrom T N *et al* 1996 *Phys. Plasmas* **3** 1867
[54] Zohm H 1996 *Plasma Phys. Control. Fusion* **38** 105
[55] Groebner R J *et al* 1996 *Plasma Phys. Control. Fusion* **38** 1249
[56] Noterdaeme J-M *et al* 2003 *Nucl. Fusion* **43** 274
[57] Rice J E *et al* 1998 *Nucl. Fusion* **38** 75
[58] Chan V S *et al* 1999 *Proc. 13th Topical Conf. on Radio Frequency Power in Plasmas (Maryland)* 45
[59] deGrassie J S *et al* 1999 *Proc. 26th EPS Conf. on Controlled Fusion and Plasma Physics (Maastricht)* **23J** 1189
[60] Rozhansky V *et al* 2006, *Modeling of radial electric field profile for different divertor configurations*, submitted to *Plasma Phys. Control. Fusion*
[61] Saibene G *et al* 2002 *Plasma Phys. Control. Fusion* **44** 1769
[62] Taylor T S *et al* 1994 *Plasma Phys. Control. Fusion* **36** B229
[63] Boedo J *et al* 2000 *Nucl. Fusion* **40** 1397
[64] Manso M E 1993 *Plasma Phys. Control. Fusion* **35** B141
[65] Gohil P *et al* 1998 *Nucl. Fusion* **38** 93
[66] Burrell K H *et al* 2002 *Plasma Phys. Control. Fusion* **44** A253
[67] Kiviniemi T P *et al* 2001 *Plasma Phys. Control. Fusion* **43** 1103
[68] Ida K *et al* 1994 *Phys. Plasmas* **1** 116